Brillouin scattering with neutrons and recent results from the investigation of compressed gases

1991 J. Phys.: Condens. Matter 3 F73

(http://iopscience.iop.org/0953-8984/3/42/007)

J. Phys.: Condens. Matter 3 (1991) F73–F86. Printed in the UK

Brillouin scattering with neutrons and recent results from the investigation of compressed gases

Jens-Boie Suck
Institut Laue–Langevin, BP156, Avenue des Martyrs, F-38042 Grenoble Cédex, France

Received 22 May 1991

Abstract. Brillouin scattering experiments with neutrons are discussed and recent instrumental developments are presented. The most recent results of such experiments performed on compressed Ar and N_2 gases at temperatures well above the critical temperature T_c are summarized.

The results are discussed within the framework of hydrodynamic theory and it is shown that thermodynamic conditions can be found under which the newly developed experimental techniques allow to intrude into the region of pure hydrodynamics, up to now reserved for light scattering techniques. For atomic and molecular fluids a common limit between the pure hydrodynamic and the generalized hydrodynamic regimes is found between 0.25 and $0.3\,l_E Q$, where l_E is the mean free path between atomic collisions in the fluid and $\hbar Q$ is the momentum transfer. This experimentally determined limit is about a factor of two to three higher than the values of $l_E Q$ predicted by generalized Enskog theories for hard-sphere fluids.

1. Introduction

Brillouin scattering normally refers to inelastic light scattering experiments in which the photon excites or absorbs an acoustic phonon in a crystal. Owing to the wavelength of light of several hundreds of nanometres the momentum transfers $\hbar Q(=\hbar(k_0 - k)$, where $k_0 = 2\pi/\lambda_0$ and $k = 2\pi/\lambda$ are the wavevectors of the incident and the scattered particle, respectively) involved in these inelastic scattering experiments do not exceed approximately 0.04 nm^{-1}. They therefore cover a very small part of the first Brillouin zone.

Owing to the large mass of the neutron, momentum transfers coupled to the same energy transfers $\hbar\omega(=(E_0 - E)$ where E_0 and E are the energy of the neutron before and after scattering) are about two orders of magnitude larger in inelastic scattering experiments with cold and thermal neutrons compared with light scattering experiments. In neutron inelastic scattering (NIS) experiments with thermal neutrons one therefore covers a large part of reciprocal space but normally does not reach any vibrational excitations at a Q-value below 4 nm^{-1}.

For the measurement of phonon dispersion curves in crystals this limitation towards lower momentum transfers does not give rise to any inconvenience (except for very special cases), as the dispersion curves can be measured in principle in any Brillouin zone and the structure factors for scattering from phonons are more favourable in higher Brillouin zones. In the investigation of topologically disordered solids and fluids, however, it would be highly desirable if one could measure the excitations in these

0953-8984/91/420F73 + 14 $03.50

samples over a wide range of lower momentum transfers, as they are normally accessible in NIS experiments. Neutrons only couple directly to longitudinal excitations while they couple to transverse excitations via Umklapp processes outside the first Brillouin zone. Measurements in a sufficiently large energy range inside the first Brillouin zone would therefore enable a separation of the longitudinal excitations from the transverse excitations in disordered solids. In addition, the damping of excitations normally decreases with decreasing momentum transfers (e.g., as Q^2 at low Q in fluids). Excitations seen as broad humps or weak shoulders in the dynamic structure factor $S(Q, \omega)$ at larger momentum transfers can be measured as relatively sharp lines (Hafner 1983 (see figure 17)), the width of which can be determined exactly, allowing a test of the importance of the different physical processes causing the damping of the excitation. A third, at least as important, reason for all efforts to investigate the gap of momentum transfers of about two orders of magnitude between inelastic scattering experiments done with light and with thermal and cold neutrons is the fact that in the description of the dynamics of dense disordered systems (glasses, liquids, dense gases) we know only two limiting cases. The first is the limit of very low momentum transfers (very long wavelength) and low frequencies, which is described by the hydrodynamic equations, and the second is that of large momentum transfers and short times, where the collective movements of the particles can be neglected with respect to the free single-particle motion (non-interacting gas limit). Between these two limiting cases theory has to extrapolate, either by extending the free-particle limit to collective modes as is done in kinetic theories, or by extrapolating from the hydrodynamic equations, which describe the system as a continuum, towards shorter wavelengths (and larger energy transfers) where the influence of the discontinuous atomic structure becomes apparent. The NIS experiments are normally only performed in this regime of generalized hydrodynamics between the continuum and the free-particle limit. With the advent of spallation neutron sources, epithermal neutrons have become available in a sufficient amount to study the transition from the free-particle limit to the interacting particle limit even in dense samples, using incident neutron energies of several electron volts. A systematic study of the transition from hydrodynamics to the regime of generalized hydrodynamics, however, was almost impossible up to our most recent experiments, even though in two cases extension into the hydrodynamic regime have been obtained for two-momentum transfers in the case of hypercritical neon (Bell *et al* 1975) and argon (Postol and Pelizzari 1978).

At the same time this region of low momentum transfers is also very difficult to reproduce in molecular dynamics simulations, because one needs very large systems, as $Q_{\min} \sim 1/L$, where L is the linear extension of the simulated systems (e.g., Alley *et al* 1983).

For periodic crystals a reciprocal lattice exists and Brillouin zones can be defined. Topologically disordered solids and fluids do not have a reciprocal lattice. In spite of this fact it has become customary to speak about neutron Brillouin scattering experiments (NBSE) (Dorner *et al* 1976) in these systems also, if the momentum transfer involved is smaller than $\frac{1}{2}\hbar Q_p$, where $\hbar Q_p$ is the momentum transfer at which the static structure factor $S(Q)$ has its principal maximum. For simple structures the first reciprocal lattice point (Bragg peak) will appear near Q_p after crystallization of the glass or the liquid. Thus $\frac{1}{2}Q_p$ is a reasonable measure for the extension of a 'pseudo' Brillouin zone in the case of disordered matter.

2. Experimental conditions and techniques

The dynamical range of the NIS experiments performed on samples that scatter neutrons coherently—and only for such samples can the dispersion of collective modes (collective

density fluctuations) be determined—is given by the energy and momentum conservation laws, which have to be satisfied simultaneously:

$$\hbar\omega = (\hbar^2/2m)(k_0^2 - k^2) \tag{1}$$

$$\hbar Q = \hbar(k_0 - k) \tag{2a}$$

or

$$\hbar^2 Q^2 = \hbar^2(k_0^2 + k^2 - 2k_0 k\cos\theta) \tag{2b}$$

or

$$\hbar^2 Q^2 = \{E_0 + (E_0 - \hbar\omega) - 2\sqrt{[E_0(E_0 - \hbar\omega)]}^{1/2}\cos\theta\}\,2m \tag{2c}$$

where we have taken account of the fact that for isotropic scatterers like disordered solids and fluids only the modulus of the momentum transfer is of importance. Here θ is the scattering angle (the angle between k_0 and k). From the combination of the two conservation laws a condition for the incident energy E_0 of the neutron can be found, which is necessary to reach an excitation with energy $\hbar\omega$ at a momentum transfer $\hbar Q$ (e.g., Robinson 1989)

$$E_0 = \frac{\hbar^2}{4m\sin^2\theta}\left\{\left(Q^2 + \frac{2m\hbar\omega}{\hbar^2}\sin^2\theta\right) \pm \left[Q^4 - \left(\frac{2m\hbar\omega}{\hbar^2}\right)^2\sin^2\theta\right]^{1/2}\cos\theta\right\}. \tag{3a}$$

Combining this condition with a linear dispersion curve, for example, for vibrational excitations with a sound velocity v_s one arrives in the limit of low Q values at

$$E_0 = \tfrac{1}{2}mv_s^2. \tag{3b}$$

Thus the important condition in NBSE is that the velocity of the incident neutron has to be larger than the velocity of the excitation to be investigated; the sound velocity v_s in the cases discussed here. In other words, the dispersion has to be well within the dynamical range of the experiment. A reasonable choice in NBSE is $1.3\,v_s \leqslant v_0 \leqslant 1.5\,v_s$. The large range of sound velocities existing in gases, liquids and solids therefore requires spectrometers for low-angle well resolved inelastic experiments (LAWRIE spectrometers) at cold, thermal and epithermal neutron beams. As can be seen from figure 1 the ω–Q space covered with these different neutron beams are very different, only cold neutrons really allowing an approach to momentum transfer close to those achieved in light scattering experiments, while it is difficult to intrude into the Q-region below say 5 nm^{-1} with epithermal neutrons.

This necessary condition for sufficiently large incident energies is not compatible with the simultaneous condition for making measurements at low momentum transfers, as can be seen from equation (2c). Low momentum transfers relative to the momentum of the incident neutron, $Q \ll k_0$, can therefore only be achieved at the lowest values of θ, where scattering angles below 1 deg are rarely usable in NIS experiments.

It is this condition, that is to work at the smallest scattering angles, that makes NBSE so extremely difficult (and therefore unpopular). There are at least five reasons for these difficulties: at low scattering angles one works next to a *high background of the incident beam.* It was in fact the high background from the incident neutrons being scattered from the argon atoms in the argon-flushed flight path that had a major influence on the quality of the data summarized in this paper. (After many LAWRIE experiments using rather different instruments and neutron sources we are convinced that really good

experiments of this type can only be done if neutrons between the primary spectrometer and the detector can be exclusively scattered by the monitor and the sample.

To enable work to be done at low scattering angles and with a good Q-resolution the incident beam has to be *strongly collimated*, which greatly reduces the intensity of the incident neutron beam.

At low Q the coherently scattering samples scatter virtually no neutrons (see $S(Q)$ at low Q). Thus one is left with only a few *single scattering events* from the sample. For samples with a large compressibility as is the case for fluids near their critical point this limitation is less severe because $S(Q = 0) = X_T/X_T^0$, where X_T is the isothermal compressibility of the fluid and X_T^0 that of the ideal gas. One therefore has to work with unusually strongly scattering samples in order to obtain any single-scattered intensity at all. In fact, in the cases described here we have been using samples that scattered 20 to 40% of the incident neutrons, quite in contrast to the 10% scatterers used in normal NIS experiments.

As a consequence the low intensity of single-scattered neutrons contrasts with the high intensity of *multiple-scattered neutrons*, because in multiple scattering processes the Q-values at scattering angles up to 180° (the 'Z' trajectory in the sample) are considerably larger than in single scattering processes and one can therefore pick up much higher intensities (see $S(Q)$ at higher momentum transfers). This effect plays a very important role in LAWRIE experiments performed with thermal and epithermal neutrons. For cold neutrons the momentum transfer even in backscattering remains well below Q_p and the intensity of multiple-scattered neutrons is therefore small and structureless—an important advantage for the experiments on compressed gases described here. Thus one finally ends up with weak single scattering processes against a high background from the incident beam and from multiple-scattered neutrons.

At the same time the requirement for *ω- and Q-resolution* are rather high and one needs both of them: the very good ω-resolution in order to be able to separate the Brillouin peaks from the Rayleigh line and to measure their width accurately, and the good Q-resolution in order to follow the change of the dispersion curve with momentum transfer. Stringent resolution requirements can again only be satisfied by a drastic loss of the incident intensity, reducing further the number of neutrons on the sample. In the cases summarized here, the energy resolution (measured at $\hbar\omega = 0$) was approximately 70 μeV, depending on the incident energy chosen. The resolution in momentum transfers was better than 0.5 nm^{-1}.

NBSE have mainly been carried out on triple-axis spectrometers (TAS) so far. The extreme requirements of these experiments necessitate the installation of very large helium-flushed flight paths between monochromator and analyser, thus depriving the TAS of one of its greatest advantages, its flexibility, and making precise positioning slower and more difficult. Because of the very tight collimation (10–20 minutes) necessary to meet the resolution requirements and to reach scattering angles of 1 to 2°, the background conditions are very favourable; however, the measurements are very time consuming for the reason mentioned above and because one obtains one value of $S(Q, \omega)$ at a time. One measures the scattered intensity at constant momentum transfer; however, it is difficult to convert this intensity into absolute values of the dynamical structure factor (especially if one works with $k_0 =$ constant, which is often necessary because of the inflexible set up), because every point in ω–Q space is measured with a different spectrometer setting (different experimental parameters), of which the changing reflectivity of the analyser and the changing number of multiple-scattered neutrons transmitted to the detector are not easily corrected for. In addition, focusing effects in

reciprocal space can change quite considerably the energy resolution in going from the neutron energy gain to the neutron energy loss side of the spectrum (see, e.g., Söderström *et al* 1980).

Alternatively, time-of-flight (TOF) instruments have been used in a few cases with rather impressive results (e.g., Copley and Rowe 1974, Postol and Pelizzari 1978). Many of the disadvantages mentioned in connection with TAS experiments do not exist in TOF experiments, as no experimental parameter is changed during the experiment, all accessible values of $S(Q, \omega)$ are measured simultaneously, and all intensities scattered into one Debye–Scherrer cone can be summed up without loss of information from the isotropic sample. Thus absolute values of $S(Q, \omega)$ can be easily determined if the measurements at constant scattering angles θ have been done on a sufficiently dense grid in ω–Q space, including all corrections for multiple-scattered neutrons and the smoothly varying resolution function of the spectrometer, as has also been done with the data summarized below. Conventional TOF spectrometers have, however, at least two clear disadvantages compared with TAS: the high background from the incident neutron beam normally prevents measurements below 3° (and most of the existing TOF spectrometers are therefore not equipped with really low scattering angle detectors—linear detectors, except for arrays of linear position-sensitive devices (PSD), not being useful at low scattering angles because of the poor Q-resolution they provide) and on most of the existing TOF spectrometers it is very difficult if not impossible to change the resolution in energy and momentum transfer from the conventional 3 to 8% to the mostly required resolution of 1 to 2%.

In view of this background of experiences it seemed necessary to set up a new spectrometer, adapted to the special requirements of LAWRIE (Egelstaff *et al* 1989). This spectrometer consists of the primary spectrometer of a TOF spectrometer with sufficiently good primary resolution and a well collimated beam and of a small-angle neutron scattering (SANS) diffractometer with evacuated flight path (in order to reduce the background from the incident beam) between the primary spectrometer and the position-sensitive (x–y) detector. The experiments discussed below have still been done with the argon flushed flight path instead of with an evacuated one, which caused considerable problems with background. As from each of the 64 × 64 cells of the PSD one TOF spectrum with 512 time channels would be obtained, the information consisting of 20 bits before the combined SANS and TOF electronics had to be reduced. For isotropically scattering samples this can be easily done by adding up all the detector cells on concentric rings around the incident beam before the signal reaches the TOF analysing unit, thus collecting the maximum intensity possible at each scattering angle and, at the same time, maximizing the Q-resolution on the detector side. This is the real advantage of this new type of spectrometer compared with traditional TOF spectrometers. For anisotropic scatterers sections of rings have to be chosen. In order to cover a range of momentum transfers as large as possible, the detector centre was displaced with respect to the incident beam by a quarter of the diameter of the detector, this choice giving a fairly homogeneous effective efficiency of the detector over its diameter. The same type of LAWRIE spectrometer will soon be set up on one of the thermal beam tubes at the high-flux reactor (HFR) at the ILL in Grenoble and possibly at some time in the future also at a spallation source, which will enable experiments with epithermal neutrons in samples with high sound velocities.

3. Theoretical background

The vibrational dynamics of fluids and solids in the limit of long wavelengths and low frequencies is described by the laws of hydrodynamics, a continuum theory, which

therefore does not take into account the atomic structure of the samples. Thus the wavelength of the excitation has to be large with respect to the atomic dimensions if the hydrodynamic laws are to hold.

Hydrodynamic theory (see Boon and Yip 1980) is based on the three conservation laws of matter or particle density, of momentum or velocity density, and of energy density. If for the momentum conservation equation the Navier–Stokes equation is used, and if in the energy conservation equation the Fourier law (linear response) for the heat conductivity is taken, and if the three conservation equations are linearized, that is all fluctuations in ρ, v and T are assumed to be small, then one arrives at three linearized hydrodynamic equations (the conservation laws) from which the dispersion relation of the hydrodynamic modes can be calculated. One thus obtains five hydrodynamic modes, of which three are longitudinal and two are transverse. For neutron scattering from fluids the three longitudinal modes are of importance.

Usually the linearized hydrodynamic equations are simplified one step further in the derivation of the dispersion relation in keeping only terms up to Q^2 in a first-order perturbation calculation. In this approximation the diagonalization of the dispersion equation gives three longitudinal modes, one at $\hbar\omega = 0$, the Rayleigh line, describing entropy fluctuations at constant pressure and two modes at $\hbar\omega = \pm cQ$, the Brillouin lines, which describe pressure fluctuations at constant entropy, that is the excitation and absorption of the longitudinal long-wavelength sound modes with sound velocity c. The dynamical structure factor $S(Q, \omega)$ divided by the static structure factor $S(Q)$ consists therefore of three Lorentz lines, of which the two Brillouin lines are modulated by an S-shaped curve, with the consequence that the frequency moments up to the second are finite:

$$\frac{S(Q,\omega)}{S(Q)} = \frac{1}{2\pi\gamma}\left[(\gamma-1)\frac{2\Gamma_T}{\omega^2+\Gamma_T^2} + \frac{\Gamma_s}{(\omega+cQ)^2+\Gamma_s^2} + \frac{\Gamma_s}{(\omega-cQ)^2+\Gamma_s^2}\right.$$
$$\left. + \left(\frac{\Gamma_s}{Q^2} + (\gamma-1)\frac{\Gamma_T}{Q^2}\right)\frac{Q}{c}\left(\frac{\omega+cQ}{(\omega+cQ)^2+\Gamma_s^2} - \frac{\omega-cQ}{(\omega-cQ)^2-\Gamma_s^2}\right)\right]. \tag{4}$$

Here $\gamma = C_p/C_v$ is the ratio of the specific heats measured at constant pressure and at constant volume, $\Gamma_T = Q^2 D_T = Q^2(\lambda/\rho C_p)$ is the thermal diffusivity multiplied by Q^2, which describes the attenuation of the entropy fluctuations (at constant pressure), that is the width of the Rayleigh line, λ is the thermal conductivity and ρ the density of the sample.

$$\Gamma_s = \Gamma Q^2 = \tfrac{1}{2}Q^2[\nu_\ell + (\gamma-1)D_T]$$

describes the attenuation of the sound modes, that is the width of the Brillouin lines.

In the hydrodynamic limit all the parameters entering equation (4) are *constants* and have been obtained from the published literature (e.g., Hoheisel and Luo 1990) except for the longitudinal kinematic viscosity

$$\nu_\ell = (\tfrac{4}{3}\eta + \eta_B)/\rho.$$

This was therefore either fitted by taking a constant mean value over all the values obtained for different Q-values or was calculated using the ratio of η to η_B given in the generalized Enshog theory (Kamgar-Parsi *et al* 1987). Here η is the shear viscosity and η_B is the bulk viscosity.

If the experimental conditions are such that the pure hydrodynamic description of $S(Q, \omega)$ is no longer applicable, the general structure of this equation can still be maintained, but the parameters then start to depend on momentum transfer and generally also on the energy transfer. Equations derived from equation (4) with Q- (and ω-) dependent parameters are called *generalized hydrodynamic equations*. It is these equations that apply to the normal NIS experiments done on fluids. The basic questions in connection with these NBS experiments were therefore as follows.

(1) Can one reach the region of validity of pure linearized hydrodynamics in neutron scattering experiments at all?

(2) Can one investigate this region in a systematic manner?

(3) Can one define and study a limiting region between that of pure and generalized hydrodynamics?

Once the exact equation for $S(Q, \omega)$ is known in the hydrodynamic limit, one can also start from more general models for the dynamics of fluids and reduce them to the hydrodynamic limit.

Kinetic theory can be extrapolated from the opposite limit, the free-particle limit, described by the Boltzmann or more generally the Enskog equation towards the ω–Q region where collective atomic movements, and finally hydrodynamic modes, dominate the fluid dynamics (de Schepper and Cohen 1980, 1982). In this case the—in principle—infinitely many kinetic modes, each described by a Lorentzian, reduce to three hydrodynamic and two kinetic modes in the transition region to the hydrodynamic regime. $S(Q, \omega)$ therefore can be represented by three (or five) Lorentzians (see, e.g., Bafile *et al* 1990)

$$\frac{S(Q,\omega)}{S(Q)} = \frac{1}{\pi}\operatorname{Re}\left(\sum_{j=-1}^{1}\frac{A_j}{\mathrm{i}\omega - z_j}\right) = \frac{1}{\pi}\left(A_0\frac{Z_T}{\omega^2+Z_T^2} + A_s\frac{Z_s+(\omega+\omega_s)b}{(\omega+\omega_s)^2+Z_s^2}\right.$$
$$\left. + A_s\frac{Z_s-(\omega-\omega_s)b}{(\omega-\omega_s)^2+Z_s^2}\right) \tag{5}$$

where the parameters Z_T, Z_s, $r = A_0/A_s$ and ω_s are *Q-dependent*. Here

$$b = \omega_s^{-1}((r/2)Z_T + Z_s) \quad \text{and} \quad A_s = \operatorname{Re} A_{+1}.$$

If the parameters determining the width of the Lorentzian at $\hbar\omega = 0$ and at $\pm\omega_s$ are small compared with the separation ω_s of the side peak, that is one has three well defined (Lorentzian) peaks, equation (5) can be transformed to equation (4) in setting

$$\begin{aligned} &A_0 = (\gamma-1)/\gamma \qquad A_s = 1/2\gamma \\ &\omega_s = cQ \qquad Z_T = D_T Q^2 = \Gamma_T \quad \text{and} \quad Z_s = \Gamma Q^2 = \Gamma_s \end{aligned} \tag{6}$$

with all other quantities having been defined in connection with equation (4). Thus equation (5), with the parameters defined in equation (6), applies to the hydrodynamic limit, as long as the parameters in equation (6) are kept constant. The results obtained for fluid argon, discussed below, have been fitted with equation (5) (Bafile *et al* 1990), however, leaving the parameters dependent on Q, which is equivalent to the generalization of equation (4) to generalized hydrodynamics.

A third possibility to arrive at the description of the dynamics of a fluid in the hydrodynamic limit is the reduction of the memory function approach, which describes the dynamics of a fluid in the generalized hydrodynamic regime (see Boon and Yip 1980)

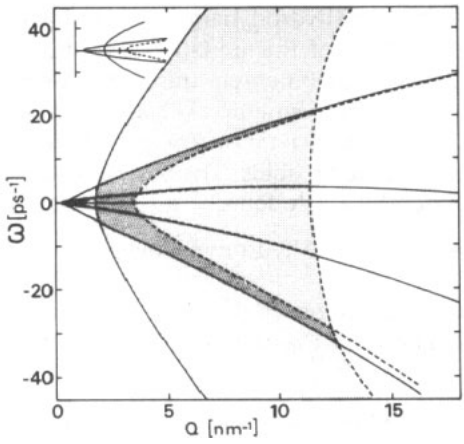

Figure 1. ω–Q space covered in time-of-flight experiments with scattering angles between 1 and 6° and three different incident energies: 2.5 meV (cold neutrons, black region), 25 meV (thermal neutrons, dark grey region) and 250 meV (epithermal neutrons, light grey region). In the inset the lowest accessible Q-region is augmented by a factor of two.

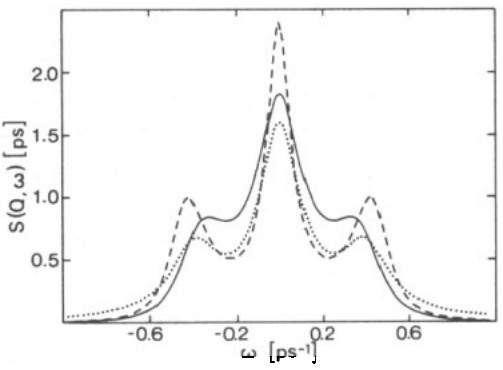

Figure 2. The dynamic structure factor $S(Q, \omega)$ normalized by its zeroth-moment calculated for fluid argon at 300 K and a density of 5 atoms/nm^3 with linearized hydrodynamics (full curve), the sum of three Lorentzians (dotted curve), that is omitting the S-shaped terms in equation (4) and with the memory function approach with $S(Q) = S(0)$ in ω_0^2 and $\tau_M = 0$ (broken curve).

to an equation appropriate for the description of pure hydrodynamics. In this case, the real and imaginary parts of the memory function $M(Q, \omega)$ in the general equation for the dynamic structure factor

$$\frac{S(Q,\omega)}{S(Q)} = \frac{1}{\pi} \frac{\omega_0^2 Q^2 M'(Q,\omega)}{[\omega^2 - \omega_0^2 + \omega Q^2 M''(Q,\omega)]^2 + [\omega Q^2 M'(Q,\omega)]^2} \tag{7}$$

have to be defined in such a way as to comply with the hydrodynamic limit. This is achieved by setting

$$\mathrm{Re}\{M(Q,\omega)\} = M'(Q,\omega) = \frac{1}{\gamma}\frac{(\gamma-1)c^2\Gamma_T}{(\omega^2+\Gamma_T^2)} + \frac{\nu_l}{1+(\omega^2\tau_m^2)}$$

and

$$\mathrm{Im}\{M(Q,\omega)\} = M''(Q,\omega) = -\frac{1}{\gamma}\frac{(\gamma-1)\omega c^2}{(\omega^2+\Gamma_T^2)} - \left[\frac{\nu_l \omega \tau_m}{1+\omega^2\tau_M^2}\right] \tag{8}$$

where $\omega_0^2 = k_B T Q^2/MS(0)$ and τ_M is the Maxwellian relaxation time describing the relaxation of the longitudinal kinematic viscosity. Therefore τ_M does not enter equation (7) in the hydrodynamic limit ($\tau_M = 0$), but has been added here as a second step in the generalization of the hydrodynamic equation, which is (7) and (8) without the terms in the square brackets, the first step in the generalization being the replacement of $S(0)$ by $S(Q)$ in ω_0^2. Here k_B is the Boltzmann constant and M the mass of the scatterer, which does not enter equations (4) to (6) and ω_0^2 is the second frequency moment of $S(Q, \omega)$ normalized by the $S(0)$ zeroth moment at $Q = 0$. All other parameters have been defined in connection with equation (4). Equations (7) and (8) are equivalent to equation (4) as long as all the parameters are kept constant, $S(0)$ is used in ω_0^2 and $\tau_M = 0$.

This memory approach, which does not presuppose sharp well separated Brillouin peaks, has been used in the form of equations (7) and (8) with constant parameters to fit the data obtained for fluid N_2 (Youden 1991), and some of the fluid ^{36}Ar spectra, however, with $\tau_m \neq 0$ and in some cases replacing $S(0)$ in ω_0^2 by $S(Q)$. The fixed parameters were either obtained from the literature or in the case of ν_ℓ and τ_m by a fit of the data leaving ν_ℓ and τ_m as free parameters and finally taking a constant mean value over all the values obtained at different momentum transfers. Figure 2 gives an example for each of the three approaches discussed here for the case of ^{36}Ar at 300 K and a pressure of 20 MPa. Kinetic theory (dotted curve) is presented here by three Lorentzians without the S-shape asymmetry term. This term moves the Brillouin peaks nearer to the Rayleigh line and narrows the spectrum as can be seen for the full curve (linearized hydrodynamics as given by (4)). The memory function approach (broken curve) shows the most pronounced peaks with peak positions very near the three-Lorentzian model, but with a considerbly faster decrease to larger energy transfers.

4. Discussion of recent experimental results

In the following the two most recent experiments performed on the LAWRIE spectrometer option installed on the cold-neutron TOF spectrometer IN5 at the HFR of the ILL in Grenoble are discussed. Both systems, ^{36}Ar and N_2, were measured at room temperature, that is well above their critical temperatures, in order to be able to vary the number density by factors of two and more with moderate pressure changes. The system ^{36}Ar was measured at pressures of 2, 5, 8 and 20 MPa, that is at 0.49, 1.23, 2 and 5.04 atoms nm^{-3}. The lower density data could be measured because of the exceptionally high coherent scattering cross section of 77.9 b for ^{36}Ar, but these data will not be discussed here as they are presented in a separate contribution (Bafile *et al* 1991a, b). The wavelength of the incident neutrons λ_0 was 0.6 nm and scattering angles between 1.3° and 7.2° were covered by the displaced detector setting described in section 2. Thus momentum transfers between 0.3 to 1.3 nm^{-1} and an energy range of $\omega \simeq \pm 1$ ps^{-1} were covered.

N_2 was measured at 27.3 and 46 MPa, corresponding to densities of 5.9 and 8.5 molecules nm^{-3}. As the sound velocity changes with density, the wavelength of the incident neutrons was reduced from 0.56 to 0.5 nm when the pressure was raised to 46 MPa. Otherwise the same experimental parameters were used as in the ^{36}Ar experiment except that the N_2 fluid at higher pressure was in a stainless-steel cell, while otherwise pressure cells with plain thick sapphire windows were used. All necessary corrections, including those of multiple scattering and for the finite resolution of the spectrometer were applied to the ^{36}Ar data, while no resolution correction was applied to the N_2 data. Instead, the calculated model for $S(Q, \omega)$ (cf. equation (7)) was convoluted with the known triangular resolution function of the spectrometer IN5.

Figure 3 shows two cuts at $Q = 0.75$ and $Q = 1.25$ nm^{-1} through the dynamic structure factors of ^{36}Ar, normalized by the integrated dynamic structure factor at a density of 5.04 (left-hand side) and of 2 atoms nm^{-3}. The experimental data (see Bafile *et al* 1990) at the higher density are compared with linearized hydrodynamic theory (broken curve) as derived from the memory function approach (equation (7)) with no adjustable parameter except that the experimental and theoretical curves are normalized to the same surface (zeroth-frequency moment) (Youden 1991). Only at the highest momentum transfers does linearized hydrodynamics deviate from the measured data. At all Q-values, including the largest, generalized hydrodynamics (equation (7)), that is linearized hydrodynamics plus a fixed Maxwellian relaxation time of 1.4 meV^{-1}, describes

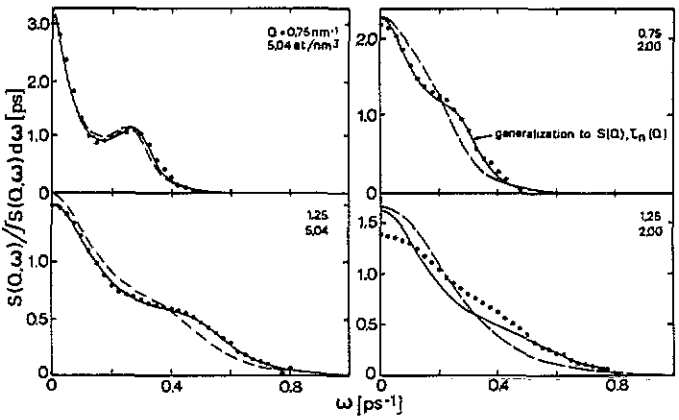

Figure 3. Cuts through the dynamic structure factor (normalized by its zeroth moment) for ^{36}Ar measured at 303 K and a density of 5.04 atoms nm^{-3} (left-hand side) and 2 atoms nm^{-3} (right-hand side) at $Q = 0.75$ and 1.25 nm^{-1}. The experimental data are compared with linearized hydrodynamic theory in the form of the memory function approach given in equation (7) (broken curves) and the generalization of this equation to constant values of $S(Q) \neq S(0)$ and $\tau_M \neq 0$ (full curves). Only 2 of the 19 cuts between 0.3 and 1.3 nm^{-1} are shown here. While the data at lower Q and higher density are well described by hydrodynamic theory, this theory is not applicable to the experimental results taken at the highest momentum transfers and at the lower densities.

the data very well. This is by no means the case for ^{36}Ar at the lower density measured in the same region of momentum transfers. Figure 3 (right-hand side) demonstrates the inadequacies of both theoretical approaches, even if in addition to generalizing the linearized hydrodynamic theory by adding a fixed value of τ_M, $S(Q)$ in ω_0 is also now allowed to deviate from the thermodynamic limit $S(0)$. Only if these two parameters are both left as free parameters can a perfect fit of the data with equation (7) be achieved (not shown in figure 3). Both parameters now become strongly dependent on Q.

One arrives at the same conclusion as drawn here if instead of the linearized hydrodynamic theory (equation (4)) and the memory function expression (equation (7)) the kinetic theory (equation (5)) is fitted to the same data. Here the four parameters $r(Q)$ ($\frac{1}{2}r$ is the Landau–Placzek ratio), $S(Q)$, $Z_T(Q)$ and $Z_S(Q)$ have been left as free parameters in the fit of the theory to the data while c and with its ω_s and all the other parameters in the equation have been kept constant, thus starting with generalized hydrodynamics from the onset. A perfect fit of the data at both densities is obtained (see Bafile *et al* (1990)). However, plotting the Q-dependence of the free parameters one finds that for the higher density (5.04 atoms nm^{-3}) the thermodynamic parameters are constants at least up to $Q = 1$ nm^{-1}, as shown in figure 4 for the two most essential parameters (equation (6)), which describe the decay of the entropy (D_T) and pressure fluctuations (Γ) in the linearized hydrodynamic equations. For the two remaining parameters $S(Q)$ and $r(Q)$, not shown in figure 4, the same remarks apply as for D_T and Γ. The deviation of these parameters from the predictions of linearized hydrodynamics (equation (4)) (full curve for 5.04 atoms nm^{-3}, dotted curve for 2 atoms nm^{-3}) at the lowest momentum transfers is caused by an inadequate resolution correction at these lowest momentum transfers. For the results obtained for ^{36}Ar at a density of 2 atoms nm^{-3} the parameters already deviate from the predictions of linearized hydrodynamics

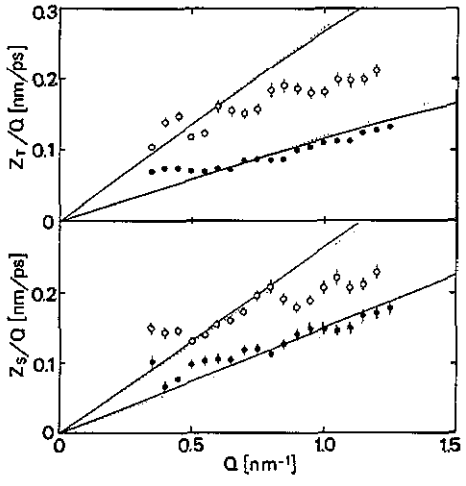

Figure 4. The Q-dependence of the Rayleigh linewidth Z_T and the Brillouin linewidth Z_S divided by the momentum transfer Q; two of the four free parameters in the fit of kinetic theory to the experimentally determined dynamic structure factor of fluid ^{36}Ar at a density of 5.04 atoms nm^{-3} (●) and 2 atoms nm^{-3} (○). The figure shows that in the case of the higher density the parameters closely follow the predictions of linearized hydrodynamic theory (full curve), at least up to $Q = 1$ nm^{-1}. Deviations at the lowest Q-values are caused by an incomplete deconvolution of the experimental data.

at small Q-values in full accordance with the differences between the measured and the calculated dynamic structure factors shown in figure 3 (right-hand side).

Thus from both types of analyses one has to conclude that for momentum tranfers, at least below 1 nm^{-1}, for the case of argon measured at 303 K and a density of 5.04 atoms nm^{-3} we have reached the hydrodynamic limit in our neutron Brillouin scattering experiment. In the same region of low momentum transfers, for lower densities the dynamics of fluid argon has to be described by one of the generalized hydrodynamic approaches and at the lowest density measured here even by theories appropriate to the free-particle limit (see Bafile *et al* 1991a, b).

Very similar conclusions can be drawn from the NBSE performed on the molecular fluid N_2. Figure 5 shows four cuts through the dynamic structure factors of N_2 at momentum transfers of 0.7 and 1.2 nm^{-1} measured at densities of 8.5 (left-hand side) and 5.9 molecules nm^{-3} (right-hand side). The experimental data are compared with the resolution-broadened linearized hydrodynamic theory in the form of equation (7) with $\tau_M \equiv 0$ using values of 12.0 and 12.3 meV Å^2 for the longitudinal kinetic viscosity for the higher and the lower density data, respectively (obtained as a mean value from a free parameter fit). Again theory and experiment are normalized to the same surface area. The comparison demonstrates that linearized hydrodynamics, that is with Q-independent parameters (Hoheisel and Luo 1990), describes the dynamic structure factor of N_2 very well at the lowest momentum transfers for both densities, doing less well for the largest Q-value shown in figure 5 in the case of the higher density, and it fails for the lower density data measured at higher momentum transfers. Thus the dynamic properties of fluid N_2 have been investigated to a large part in the limit of pure hydrodynamics in these NBS experiments, extending out into the transition region in generalized hydrodynamics.

From what has been summarized so far it is clear that it is not the absolute (small) Q-value that determines whether or not we are investigating a system in the limit of pure hydrodynamics (which has been used here as synonymous with the experimental data can be satisfactorily described by linearized hydrodynamic theory). As all the data presented here were measured in essentially the same Q-region, the answer depends on the system under investigation.

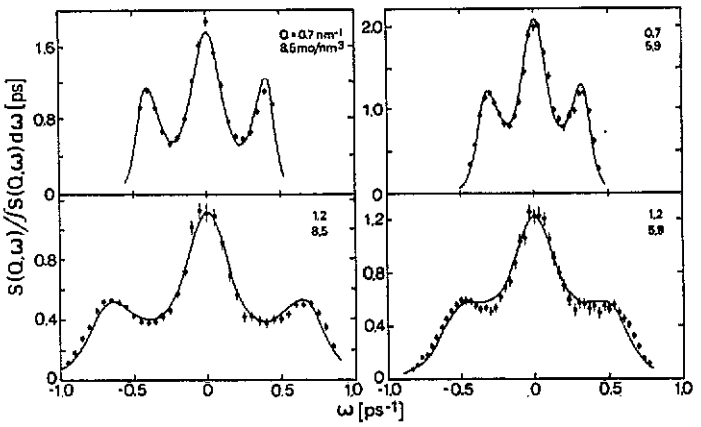

Figure 5. Cuts through the dynamic structure factor of fluid N_2 measured at 300 K and at densities of 8.5 molecules nm^{-3} (left-hand side) and 5.9 molecules nm^{-3} (right-hand side). Neutron energy gain ($\omega < 0$) and loss ($\omega > 0$) spectra are shown for momentum transfers of 0.7 and 1.2 nm^{-1}. Linearized hydrodynamics in the form of the memory function approach given in equation (7) with $\tau_M = 0$ and broadened by the resolution function of the spectrometer describes the data well except for the largest momentum transfers especially at the lower density. Only two of the nine cuts through $S(Q, \omega)$ are shown here.

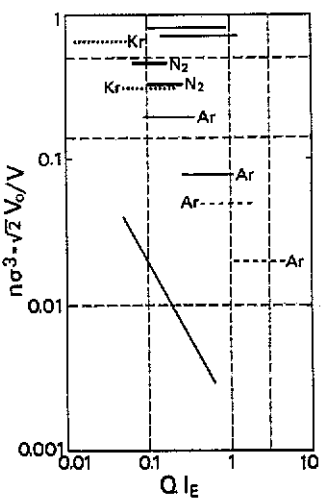

Figure 6. The 'phase diagram' for hard-sphere fluids applied to the NBSE done on Ar at 303 K and densities of 5.04, 2 (full lines), 1.43 and 0.49 atoms nm^{-3} (broken lines) and on N_2 at densities of 8.5 and 5.9 molecules nm^{-3} (bold full lines). For both systems a common transition region from the hydrodynamic to the generalized hydrodynamic description of the dynamics of these fluids can be defined for Ql_E between 0.25 and 0.3. For comparison the location of normal NIS experiments on liquid Ar, of future investigations of Kr (dotted lines) and of a light scattering experiment are also indicated in the 'phase diagram'.

An appropriate parameter for the description of the system therefore has to include some important characteristics of its state, which in this case is the *mean free path between collisions*, either in the Boltzmann $l_0 = 1/\pi\sqrt{2}n\sigma^2$ approximation or in the form given by Enskog

$$l_E = 1/\pi\sqrt{2}n\sigma^2 g(\sigma). \tag{9}$$

Here n is the number density, σ the hard-core diameter and $g(\sigma)$ the radial distribution function for hard spheres at contact.

A coherent picture of the results obtained on Ar and on N_2 in these NBSE can therefore be obtained if one plots the occupied atomic volume, normalized to the volume at dense packing (or the number density times the cube of the particle dimension), as a function of the dimensionless parameter Ql_E, which is a measure of the length of the mean free path of the atoms or molecules in the system with respect to the wavelength λ_e of an excitation associated with Q $(=2\pi/\lambda_e)$.

The resulting 'phase diagram', which has been used recently in a slightly more elaborated version to describe the results of dynamical processes in *hard-sphere* fluids using the revised Enskog theory (Kamgar-Parsi *et al* 1987), is shown in figure 6. The phase space covered in the experiments done on ^{36}Ar and N_2 are shown as full lines and full bold lines in the middle of the diagram. As l_E decreases with increasing density, experiments done in the same region of Q-values follows a diagonal from the upper left-hand corner ($\lambda_e \gg l_E$, the hydrodynamic limit) to the lower right-hand corner ($\lambda_e \ll l_E$, the free-particle limit). Normal NIS experiments on dense liquids are done in the upper middle part of the diagram, as shown for experiments on liquid argon (van Well *et al* 1985). Light scattering experiments can extend over a large range parallel to the diagonal as shown for the light scattering from compressed argon (Ghaem-Maghami and May 1980).

The NBSE described here lie approximately on the diagonal of this figure. Within this 'phase diagram' one can define an approximate common limit for the atomic (Ar) and the molecular fluid (N_2) for the transition from hydrodynamics to generalized hydrodynamics. Based on the discussion of the applicability of pure hydrodynamic theory to the measured $S(Q, \omega)$ this limit can be found to be between 0.25 and $0.3Ql_E$ for the densities discussed here. All three experiments done on ^{36}Ar at 8, 5 and 2 MPa are outside this limit and the largest part (except the highest Q-values) of the experiments done on Ar at the highest density and on N_2 at both densities lie within this limit.

This means that l_E has to be about 20 times smaller than λ_e in the fluid in order to be within the hydrodynamic region, or that about 20 collisions are needed during the time needed for the excitation to propagate by one wavelength λ_e to restore hydrodynamic conditions in the system investigated here.

The revised Enskog theory applied to hard spheres predicted this limit to be between 0.05 and $0.1Ql_E$, that is about a factor of three lower than found in our experiments. It is most probably the difference in the interaction potentials that causes this difference in the transition region.

We have shown that with a new type of spectrometer NBSE can be routinely performed down to momentum transfers an order of magnitude lower than those reached in normal NIS experiments, but still one order of magnitude higher than reached at the maximum in light scattering experiments. These experiments now enable us to investigate fluids in the hydrodynamic limit and in the transition region to generalized hydrodynamics in a systematic manner.

Acknowledgments

The experiments, the results of which were summarized here, were prepared and the data were treated in Guelph for N_2 by J P A Youden and P A Egelstaff and for Ar by U Bafile and F Barocchi in Florence and P Verkerk and L A de Graaf in Delft. I am indebted to J P A Youden for sending me the material for figures 3 and 5 prior to publication and to P Verkerk for the information for figures 4 and 6. I have in addition

profited from several discussions with P Verkerk—and from many discussions with P A Egelstaff throughout my scientific career.

References

Alley W E, Alders B J and Yip S 1983 *Phys. Rev.* A **27** 3174, 3158
Bafile U, Verkerk P, Barocchi F, de Graaf L A, Suck J-B and Mutka H 1990 *Phys. Rev. Lett.* **65** 2394
—— 1991a *Proc. Conf. on Physics of Fluids (Oxford, 1991)* (Bristol: Institute of Physics) at press
—— 1991b *Phys. Rev. Lett.* submitted
Bell H, Moeller-Wenghoffer H, Kolmar A, Stockmeyer R, Springer T and Stiller H 1975 *Phys. Rev.* A **11** 316
Boon J P and Yip S 1980 *Molecular Hydrodynamics* (New York: McGraw-Hill) ch V
Copley J R D and Rowe M 1974 *Phys. Rev.* A **9** 1656
Dorner B, Plesser Th and Stiller H 1967 *Disc. Faraday Soc.* **43** 160
Egelstaff P A, Kearley G, Suck J-B and Youden J P A 1989 *Europhys. Lett.* **10** 37
Ghaem-Maghami V and May A D 1980 *Phys. Rev.* A **22** 692, 698, 1686
Hafner J 1983 *J. Phys. C: Solid State Phys.* **16** 5773
Hoheisel C and Luo H 1990 *Nuovo Cimento* **12** D 499
Kamgar-Parsi B, Cohen E G D and de Schepper I M 1987 *Phys. Rev.* A **35** 4781
Postol T A and Pelizzari C A 1978 *Phys. Rev.* A **18** 2321
Robinson R A 1989 *Physica* B **156 & 157** 557
de Schepper I M and Cohen E G D 1980 *Phys. Rev.* A **22** 287
—— 1982 *J. Stat. Phys.* **27** 223
Söderström O, Copley J R D, Suck J-B and Dorner B 1980 *J. Phys. F: Met. Phys.* **10** L151
van Well A A, Verkerk P, de Graaf L A, Suck J-B and Copley J R D 1985 *Phys. Rev.* A **31** 3391
Youden J P A 1991 *Thesis* University of Guelph, Canada